Nucleic Acids Research, 2006, Vol. 34, No. 4 ***e32***
doi:10.1093/nar/gnj034

Controlled loading of oligodeoxyribonucleotide monolayers onto unoxidized crystalline silicon; fluorescence-based determination of the surface coverage and of the hybridization efficiency; parallel imaging of the process by Atomic Force Microscopy

Fabrizio Cattaruzza[1], Antonio Cricenti[1], Alberto Flamini[1,*], Marco Girasole[1], Giovanni Longo[1], Tommaso Prosperi[1], Giuseppina Andreano[2], Luciano Cellai[2] and Emanuele Chirivino[2]

[1]Istituto di Struttura della Materia and [2]Istituto di Cristallografia, CNR, Via Salaria Km 29,300, 00016 Monterotondo Stazione, Rome, Italy

Received November 10, 2005; Revised December 23, 2005; Accepted February 4, 2006

ABSTRACT

Unoxidized crystalline silicon, characterized by high purity, high homogeneity, sturdiness and an atomically flat surface, offers many advantages for the construction of electronic miniaturized biosensor arrays upon attachment of biomolecules (DNA, proteins or small organic compounds). This allows to study the incidence of molecular interactions through the simultaneous analysis, within a single experiment, of a number of samples containing small quantities of potential targets, in the presence of thousands of variables. A simple, accurate and robust methodology was established and is here presented, for the assembling of DNA sensors on the unoxidized, crystalline Si(100) surface, by loading controlled amounts of a monolayer DNA-probe through a two-step procedure. At first a monolayer of a spacer molecule, such as 10-undecynoic acid, was deposited, under optimized conditions, via controlled cathodic electrografting, then a synthetic DNA-probe was anchored to it, through amidation in aqueous solution. The surface coverage of several DNA-probes and the control of their efficiency in recognizing a complementary target-DNA upon hybridization were evaluated by fluorescence measurements. The whole process was also monitored in parallel by Atomic Force Microscopy (AFM).

INTRODUCTION

Unoxidized crystalline silicon is considered the support of choice in nanobiotechnology (1), due to the uniformity and homogeneity of its surface at the nanometer scale (2,3) (http://public.itrs.net). However, numerous other materials, such as gold (4–22), glass (23–32), quartz (33–36), metal oxides (37), oxidized silicon (38–44), organic polymers (45–50), harbouring oligodeoxyribonucleotides (ODNs) as probes, have been much more considered for the preparation of biosensors. Related publications are, in fact, relatively few (3,51–56) and do not adequately address the following fundamental issues. First, the formation of the layer was performed through several steps in most reported cases (51–54,56), one step being an alkaline hydrolysis (52,54), which inevitably damages the silicon surface (51). Second, the quality of the cross-linking layer, spacing out the silicon surface and supporting the ODN, was controlled and optimized only in a few cases (53,56), although this feature critically influences reproducibility in using the resulting materials (3,24,28,35,41,50). Third, the probe concentration on the surface was usually not quantified, even though it is well-known that this concentration should be kept below a limiting value: 2×10^{12} strands/cm^2 according to some reports (5,16,17,22), or $4–6 \times 10^{12}$ strands/cm^2

*To whom correspondence should be addressed. Tel: +39 06 90672318; Fax: +39 06 90672316; Email: alberto.flamini@ism.cnr.it
Correspondence may also be addressed to Luciano Cellai. Tel: +39 06 90672613; Fax: +39 06 90672630; Email: luciano.cellai@ic.cnr.it

according to other reports (4,10,11), for attaining the maximum hybridization efficiency and thus for attaining the maximum sensitivity and selectivity; in fact only the hybridized target-ODN concentration was commonly reported (51–53). Fourth, the accuracy of this latter determination, achieved by solid-state fluorescence microscopy (51,52) and by electrochemistry with an external probe (53), was rather low so that the authors themselves write of 'approximate, rough values'.

In this work we present our contribution, outlined in Scheme 1, addressing the four points cited above: as reported previously (57), we have functionalized unoxidized crystalline silicon with 10-undecynoic acid (Si–COOH) in a single step procedure, obtaining a controlled monolayer of the acid. On this surface we have anchored a fluorescent-ssODN, verifying the loading upon digestion with a DNase. Alternatively, this anchored ODN was considered as a probe and hybridized with a complementary, fluorescent-ssODN, which, after repeated washing, was subsequently freed through denaturation and measured. The ODN linked on the surface was then, digested and evaluated as before, to estimate the hybridization efficiency. The whole process was monitored in parallel by Atomic Force Microscopy (AFM).

MATERIALS AND METHODS

1-(3-Dimethylaminopropyl)-3-ethylcarbodiimide hydrochloride (EDAC) and N-hydroxy succinimide (NHS) were from Fluka and used as received. All reagents used for preparing buffer solutions and Phosphodiesterase I from *Crotalus adamanteus* were from Sigma. Standard commercial reagents required for ODNs synthesis, including 3′-Amino-ON CPG columns and 5′-(6-FAM)-Fluorescein phosphoramidite were from Proligo Biochemie and Link Technologies. All ODNs were prepared on a Perseptive Biosystems Expedite 8909 automatic DNA synthesizer, using standard phosphoramidite chemistry. High-performance liquid chromatography (HPLC) was performed using a Perkin-Elmer Series 410 Bio LC pump system equipped with a Perkin-Elmer 235C Diode Array. The absorption spectra of ODNs were recorded with a Perkin-Elmer Lambda Bio 40 spectrophotometer. The concentration of the ODNs is expressed in 10^{-6} mol/l U (μM). Fluorescence measurements in solution were carried out on a Perkin-Elmer MPF-44B spectrometer. For AFM investigations, a homemade apparatus was used, as described elsewhere (58).

Silicon surface activation and functionalization with 10-undecynoic acid

Single-side polished n-Si wafers (from Siltronix, phosphorus-doped, 0.1–0.01 Ω cm resistivity, (100) orientation, 1 inch diameter, 500 μm thickness) were first washed in boiling 1,1,2-trichloroethene for 10 min and subsequently in methanol at room temperature, with sonication for 5 min. They were then oxidized in H_2O_2 (30%)/HCl (37%)/H_2O (2:1:8) at 80°C for 15 min, repeatedly rinsed with water, etched with 10% aqueous HF for 10 min, rinsed with water again, dried through a stream of N_2 and immediately closed in a dry-box to undergo the functionalization process. The functionalization with 10-undecynoic acid was performed via cathodic electrografting (CEG), according to the procedure reported previously (57). In details, this CEG process was carried out at constant intensity current (0.6 mA) in a two compartment polyethylene cell. The working electrode was the silicon wafer with 1.5 cm^2 exposed area, in a CH_3CN solution (3.5 ml) of 10-undecynoic acid 0.1 M and tetraethylammonium perchlorate (TEAP) 0.1 M as the supporting electrolyte. An ohmic contact on the rear side of the silicon was established after scratching the surface, rubbing it with Ga-In eutectic and attaching a copper contact to it. The electrode set-up was obtained by pressing the silicon wafer against an O-ring sealing a calibrated hole in the bottom of the cell. The counter electrode was a Pt-coil in a 3 ml solution of TEAP 0.1 M in CH_3CN, filling a glass tube separated from the working compartment by a glass sintered disc (porosity 3). Several samples were prepared varying the total amount of faradaic charge (Q), passed during CEG.

Preparation of ODNs

The ODNs (Table 1, **1**–**8**) were prepared at the 1 μmol scale and, having used Tac-protected dC (Proligo), were cleaved

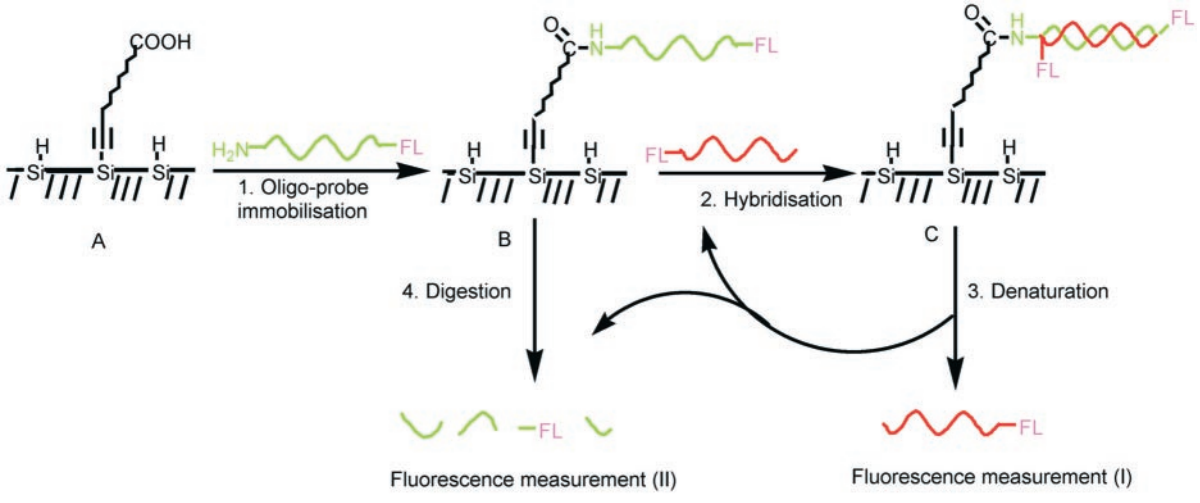

Scheme 1. Overall procedure.

from the solid support by a mixture of ammonia and methylamine (AMA, Beckmann) in 10 min at room temperature, then the solution was heated for 10 min at 55°C. After removing AMA by rotating evaporation under vacuum (Speed Vac, Savant), the samples were dissolved in triethylammonium acetate 0.1 M (pH 7.0) buffer (TEAA) and purified on an HPLC column Vydac C18, 300 Å, 5μ, 50 × 22 mm, eluted at a flow-rate of 6 ml/min with a linear gradient 3–45% MeCN in TEAA 0.1 M (pH 7.0), in 20 min. The ODNs were further purified by HPLC on a SAX Dionex Nucleopack100, 250 × 22 mm column, with a slightly concave gradient 10–30% of $NaClO_4$ 0.5 M in Tris–HCl 25 mM buffer (pH 8), in 15 min, at a flow-rate 9.0 ml/min, then lyophilized and desalted on the Vydac column as above, but replacing TEAA with water. The ODNs were analysed on a SAX Dionex Nucleopack100, 250 × 4 mm column, with the same gradient as above, at a flow-rate 1.5 ml/min. The ssODNs were also analysed by PAGE on 15% polyacrylamide, 7 M urea gels (1 mm), containing 50 mM Tris–borate (pH 8.0), 0.1 mM EDTA buffer (Sigma), staining with ethidium bromide. The dsODNs were analysed both by HPLC and PAGE under analogous conditions as above, but omitting urea in PAGE.

Immobilization of ODNs

Unoxidized, crystalline silicon samples, pre-functionalized with undecynoic acid, were immersed in 4 ml phosphate buffer [Na_2HPO_4/NaH_2PO_4 (pH 6.84)] containing variable concentration of ODN (ca. 30–0.5 μM), EDAC 0.026 M and NHS 0.0017 M and let react overnight at room temperature. Afterwards, the solution was removed and silicon was cleaned by sonicating two times for 20 min with phosphate buffer and two times for 20 min with NaH_2PO_4 20 mM, NaCl 300 mM, EDTA 2 mM, SDS 7 mM (SPPE) and then rinsed thoroughly with SPPE at 60°C until the discarded solution was no longer fluorescent. The incubation time proved suitable to attain the thermodynamic equilibrium of the loading on to the Si⊢COOH substrate. ODN **2** was chosen as test-probe; different surface loading values were obtained depending on the ODN concentration in solution (Table 2). The other ODNs used as probes (**1**,**5**,**7**) were anchored after selecting the appropriate conditions, based on the results for ODN **2** (see below).

Fluorescence measurement calibration

The concentration of the ODNs in solution was calculated using the extinction coefficient derived from the Oligonucleotide Properties Calculator (www.basic.northwestern.edu/biotools/oligocalc.html), assuming that the presence of the linker arm does not influence the ODNs optical properties.

Table 1. List of oligodeoxynucleotides

1 Fluorescein-5′-dA_{20}-3′-Hexyl-NH_2
2 Fluorescein-5′-dT_{20}-3′-Hexyl-NH_2
3 Fluorescein-5′-dA_{20}-3′
4 Fluorescein-5′-dT_{20}-3′
5 Fluorescein-5′-d(GCCTGGCTAGGTGACGAGCT)-3′-Hexyl-NH_2
6 Fluorescein-5′-d(AGCTCGTCACCTAGCCAGGC)-3′
7 Fluorescein-5′-d(GCATCATACGATATCCATG ACGAGTGACCGTCGAGAGGTCACACGAGTCTG)-3′-Hexyl-NH_2
8 Fluorescein-5′-d(GTCATGGATATCGTATGATGC)-3′

Given the fact that the fluorescence quantum yield of fluorescein is dependent on the substrate to which it is bound (59), then the corresponding fluorescence calibration plot was determined for each fluorescein-labelled ODN used in this study (Table 1, **1**–**8**). Fluorescence intensity (λ_{ex} = 492 nm, λ_{em} = 520 nm) was measured twice on five samples at concentrations in the range 0.5–6.0 × 10^{-9} M, prepared from 10^{-4} M stock solutions of each ODN, either in the digestion buffer (Tris–HCl), after digestion of the ODN with Phosphodiesterase I (**1**,**2**,**5**,**7**), or in 7 M urea (**3**,**4**,**6**,**8**), i.e. the expected solution composition and range of measurement. Two typical, slightly different trends, namely of ODN **2** and **3**, in Tris–HCl buffer after enzymatic digestion and 7 M urea, respectively, are reported here (Figure 1). They are both linear, expressed by the equations 1.10 + 7.34(x) and 2.96 + 6.55(x), with associated correlation indexes 0.9744 and 0.9933, resulted by application of least-squares fitting, including the origin as an experimental point. Using these calibration plots, the approximation on fluorescein determination is ca. 0.10 × 10^{-9} M, and thus the limit of detection (LOD) of fluorescein in

Table 2. Density of the ODN-probe **2** immobilized on the silicon surface (1.5 cm^2 exposed area) as function of its concentration in solution[a]

ODN concentration in solution (μM)	ODN density on silicon surface (10^{12} strands/cm^2)	Hybridization efficiency %[b]
27.135	8.10	40
13.567	9.44	73
2.714	6.54	92
0.543	5.64	100
0.135	2.09	100

[a]Reaction conditions: 4 ml phosphate buffer plus EDAC 0.026 M and NHS 0.0017 M; overnight; room temperature.
[b]After hybridization, denaturation and fluorescence measurements in solution (see text).

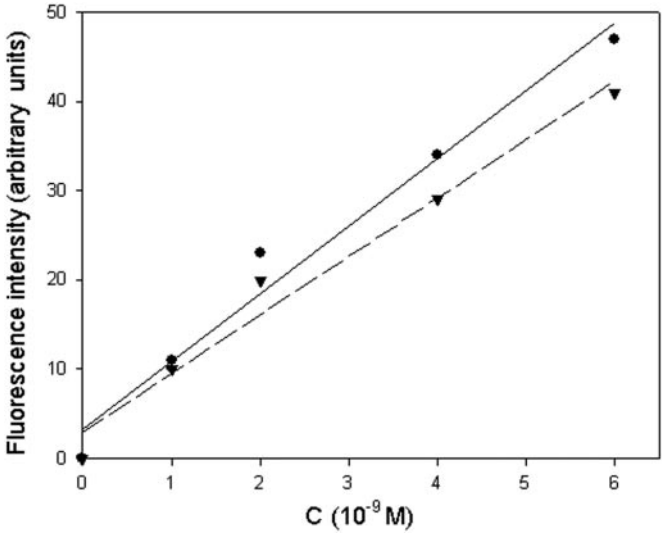

Figure 1. Dependence of the maximum intensity emission (λ_{em} = 520 nm, λ_{ex} = 492 nm) of ODN **2** Fluorescein-5′-dT_{20}-3′-Hexyl-NH_2 on its concentration in Tris–HCl buffer after digestion with Phosphodiesterase I (straight line, closed circle) and of **1** ODN Fluorescein-5′-dA_{20}-3′ in urea 7 M (dashed line, closed inverted triangle).

solution is ca. 0.30×10^{-9} M, equivalent to 1.2×10^{-12} mol, for a measurement volume of 4 ml. By considering that such two-dimensional ODN-monolayers, fully covering the planar support, have a density of 6×10^{-11} mol/cm^2 (60), this method allows to detect a submonolayer lower than 2.0%, provided that the area of the functionalized silicon surface is $\geqslant$ 1.0 cm^2 and the volume of the solution is $\leqslant$4 ml. The calibration plot equations for the other cases are the following: $0.87 + 9.82(x)$, $3.28 + 7.59(x)$, $-0.60 + 1.77(x)$ and $-2.72 + 7.20(x)$ for ODN **1**, **2**, **5** and **7** in Tris–HCL buffer; $2.53 + 9.95(x)$, $0.32 + 2.64(x)$ and $-2.34 + 10.13(x)$ for ODN **1**, **5** and **7** in the same buffer but after the enzymatic digestion; $-0.422 + 1.01(x)$, $2.10 + 4.34(x)$ and $1.37 + 5.32(x)$ for ODN **4**, **6** and **8** in urea 7 M.

Evaluation of the anchored ODNs

The enzymatic degradation of the probe-ODNs present on the silicon surface was accomplished by immersing the sample in 4 ml of KH_2PO_4 10 mM, 10 mM $MgCl_2$-$6H_2O$ (pH 7.0), adding 4 mU of Phosphodiesterase I, leaving for 6–24 h at 40°C, following digestion kinetics up to apparent completion through fluorescence measurements. The results for ODN **2** are reported in Figure 2.

T_m measurements

The ability to hybridize of the free, modified complementary ssODNs (**1** + **4**, **2** + **3**, **5** + **6** and **7** + **8**) was monitored by heating the appropriate equimolar mixtures (2.7–0.9 μM) in NaH_2PO_4 10 mM, NaCl 100 mM, EDTA 0.1 mM (pH 7.2), at 95°C for 2 min and allowing them to reach slowly r.t. Thermal denaturation curves were then obtained by monitoring the absorbance of the pre-hybridized ODNs at 260 nm as a function of temperature with a Perkin-Elmer 330 spectrometer, equipped with a Peltier temperature control accessory, in a stoppered 1 cm path length couvette. A ramp rate of 1°C/min with a hold time of 1 min was used over the range 25–85°C. T_m values of 44.6°C for both **1** + **4** and **2** + **3**, and 66.9°C for **5** + **6** were estimated from the inflection points of the curves obtained by plotting the collected data of absorbance versus temperature. The hybrid **7** + **8** did not show any definite inflection point, although producing a continuous increase of absorbance upon heating.

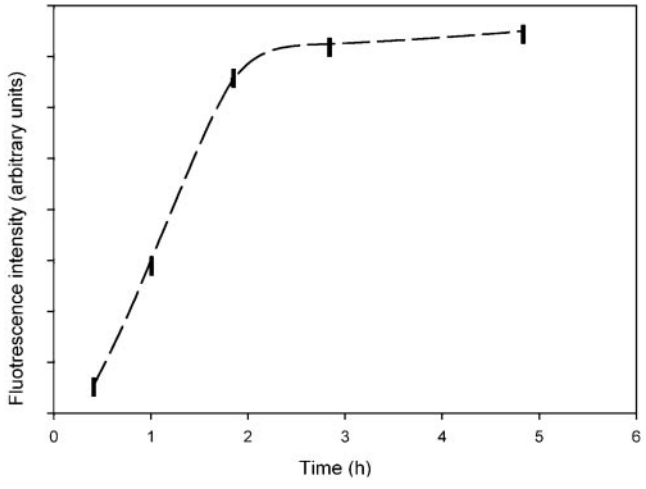

Figure 2. Solution fluorescence intensity versus time, during the enzymatic digestion of an amino-terminated oligonucleotide (**2**) immobilized on the silicon surface.

Evaluation of on-surface hybridization

The surface, derivatized with either **1**, **2**, **5** or **7** ODN, was immersed into 4 ml of ca. 10 μM hybridization solution of **4**, **3**, **6** or **8**, respectively. The system was then heated at 90°C for 5 min, slowly let cool down to room temperature, and left for 1 h at 5°C. Afterwards the solution was removed, the surface was repeatedly soaked into a solution of hybridization buffer and then two times for 5 min in SPPE at room temperature, until the discarded solution was no longer fluorescent, in order to remove all unbound ODN. Afterwards, denaturation of the hybrid was accomplished by immersing the sample in 4 ml of urea 7 M at 90°C, for 5 min. The solution was removed while still hot, cooled down to room temperature and analysed through fluorescence measurements. The repetition of the procedure produced no additional fluorescence. The sample was then addressed to the evaluation of ODN loading. Furthermore, the minimal amount of ODN-target in solution, which can be detected within the dynamic range accessible with this method, was determined. To this end, seven samples with immobilized ODN-probe **2** at almost the same surface density ($5.64–5.87 \times 10^{12}$ strands/cm^2) were prepared and hybridized with the ODN-target **3** at a variable solution concentration (10.615–0.312 μM). The obtained results are reported in Table 3.

AFM imaging

AFM images, were taken in different areas of every sample in order to characterize the quality of each step of the procedure, either in the contact or in the tapping mode and all samples resulted homogenous. The measurements were performed in air, at room temperature and constant 30% relative humidity. No noise filter was applied to the raw data which were treated by only a background subtraction and, when necessary, a plane alignment. In the contact mode, the microscope works in the weak repulsive regime, with interactions between tip and sample <1 nN, allowing high resolution imaging. The images of the 10-undecynoic acid layers were taken in this way.

Moreover, the lateral scanning motion of the tip in the contact mode can be recorded through a lateral force

Table 3. Density of the ODN-target **3** hybridized[a] with the ODN-probe **2** immobilized on the silicon surface of 1.5 cm^2 exposed area[b], as function of its concentration in solution

ODN concentration in solution (μM)	ODN density on silicon surface (10^{12} strands/cm^2)
10.615	5.60
9.369	5.63
3.123	2.39
1.874	2.82
1.615	2.17
0.625	2.39
0.312	1.95

[a]Reaction conditions: 4 ml hybridization buffer, at 90°C for 5 min and then at 5°C for 1 h (see Materials and Method).
[b]ODN-probe **2** density on silicon surface for the various samples is nearly constant: $5.64–5.87 \times 10^{12}$ strands/cm^2.

(or friction force) modality that can give useful information regarding the chemical properties of the sample: different chemical properties usually imply different frictions between the sample and the scanning tip. In this case, the acquired information are qualitative and the corresponding cross section profile of the lateral force is expressed in arbitrary units (a.u.). On the other hand the contact mode operation implies forces that can produce a deformation of soft samples like ODNs on the surface. In extreme cases, the molecules could even be swept away from the surface and the particles could stick to the tip, thus damaging the sample and reducing the resolution of the measurement (61). Therefore, the ideal work regime for the analysis of the ODN covered samples is the intermittent contact mode AFM [Tapping mode AFM (62)]. In this modality, the tip oscillates on the sample with a mean interaction during a complete oscillation in the order of tens of pN, while the maximum interaction (still below 1 nN) is present only for a very small fraction of the time per oscillation and the lateral forces are strongly decreased. This allows a weak interaction with the sample, while maintaining a good lateral resolution, that depends on the choice of the tip in use.

In this work we have selected two kind of tips: standard tips with a nominal apical radius of ca. 20 nm, which have been used for most AFM contact and tapping mode images, and 'super-tips' with a nominal apical radius of 1–2 nm, which were used to determine the influence of the tip apical radius in the determination of the lateral dimensions of the imaged ODN molecules. These ultra-sharp tips have the advantage of delivering a high resolution imaging, but are expected to introduce a larger deformation on the sample, since the same force applied on a smaller area produces a higher pressure.

RESULTS AND DISCUSSION

To produce a good DNA sensor, the device should display two specific relevant properties: (i) the cross-linking layer between the surface and the ODN (the undecynoic acid layer on silicon in our case) should be deposited as a uniform monolayer and (ii) the surface density of the immobilized ODN should be high enough to ensure the highest sensitivity in the molecular recognition event, but must not exceed a value above which steric hindrance in the formation of double strands on the surface becomes relevant (63).

With regard to the first point, taking advantage of our previous studies (57), we attained a uniform monolayer modulating the faradaic charge during the CEG of the acid and controlling with AFM the resulting surfaces. Several samples were prepared varying the charge density from 1200 to 12 mC/cm^2.With 1200 mC/cm^2 the acid has deposited as multilayer, characterized by the presence of protrusions as high as 8–15 nm (Figure 3). With a 10-fold lower charge density, 120 mC/cm^2, a uniform homogeneous monolayer was formed, with typical corrugation falling between 1 and 2 nm, distinctly above the value (0.3–0.4 nm) characteristic of the clean Si(100) surface, as we reported previously (57). Then, lower charge densities of 36 and 12 mC/cm^2 were tested, in order to check whether the exposure of the silicon surface to the passage of a large charge, which can damage the surface, could be avoided. With 36 mC/cm^2 a homogeneous monolayer was obtained, practically undistinguishable from that obtained with 120 mC/cm^2. An AFM topographic image of a similar sample is presented and commented below. With 12 mC/cm^2 the silicon surface resulted characterized by a lower typical corrugation (0.9 nm) and probably only partially and non uniformly functionalized, as shown in the topographic image (Figure 4A). In order to make this point clearer, the same area was also analysed in the friction force modality, showing the formation of round patches on the surface, that appear in correspondence (see the cross section profile) to properly functionalized zones (Figure 4B).

It should be noted that, in all cases, the charge used in the CEG is in large excess with respect to the theoretical catalytic amount needed. In fact, the overall process is a redox reaction ($\equiv$Si-H + HC$\equiv$CR $\rightarrow$ $\equiv$Si-C$\equiv$CR + H_2), catalysed by the application of just a cathodic bias to the silicon surface, then a surface silyl anion is generated, which initiates a chain reaction (64). Evidently, in the chosen reaction conditions, the current efficiency of this electrocatalysed process is very low.

Valuable information regarding the characterization of the 10-undecynoic acid monolayer, came from the analysis of a tapping mode AFM image of a sample prepared by CEG of 10-undecynoic acid at 36 mC/cm^2, with the further deposition of ODN-probe **2** as explained below, which, however,

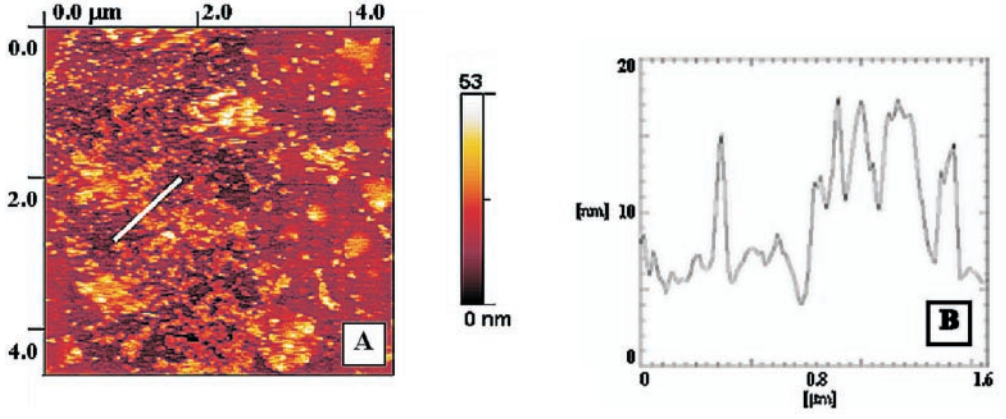

Figure 3. AFM contact mode topographic images (5 × 5 µm) of 10-undecynoic acid CEG deposited on Si(100) surface at high cathodic charge density (1200 mC/cm^2), showing non-homogeneity and aggregation (**A**). The white bar indicates the analysed zone. The cross section profile (**B**) is measured along the bar.

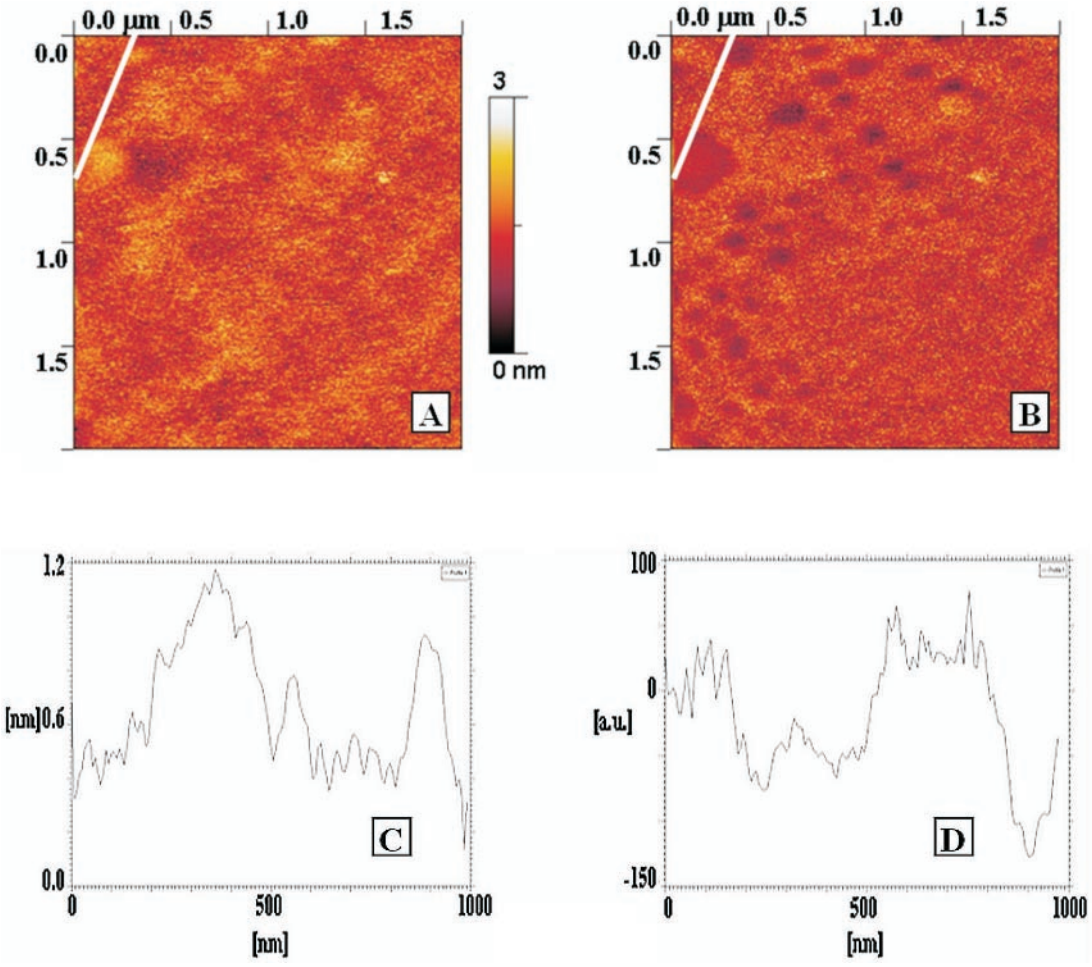

Figure 4. (**A**) AFM contact mode and (**B**) friction force topographic images (2 × 2 µm) of 10-undecynoic acid CEG deposited on Si(100) surface with at 12 mC/cm^2 cathodic charge density. The surface appears less homogeneous than as in well-covered monolayers. Round, so called 'friction holes' appear in the friction image, matching the higher areas in the contact mode topographic image. The white bar indicates the analysed zone. The corresponding cross section profiles, measured along the bar, are reported below, in (**C** and **D**), respectively.

resulted loaded in a very low amount (below the detection level by our methodology, i.e. $<5 \times 10^{11}$ strands/cm^2). The analysis of the area reported in Figure 5 allowed to better evaluate the actual thickness of the acid monolayer, evidencing well distinguished functionalized and non-functionalized areas. The ODN molecules appear as rare, sparse, round structures present on the surface, uniformly functionalized with 10-undecynoic acid and non-modified by the ODN immobilization process. The non-functionalized scratch-like area is most probably originated by the presence of some debris on the silicon surface during the functionalization, that were then removed by the cleaning procedure performed after the CEG, leaving a clean non-functionalized area. In fact, a thorough analysis of the image shows that the surface has a corrugation of 1 nm outside the scratch and only 0.3 nm inside the scratch, thus confirming the different nature of the two areas: a functionalized crystalline silicon surface with a cleft-like non-functionalized scratch. The depth of the scratch is ca. 1.5 nm, compatible with the dimension of a single layer of 10-undecynoic acid molecules, as found by other authors, who, from an analogous AFM experiment concerning the grafting of methyl 10-undecenoate on Si(100) surface, reported a depth of a scratch, done on purpose in this case, of 1.1 nm (65).

Subsequently, all other ODN-probes were immobilized on substrates all prepared by CEG of 10-undecynoic acid at Q = 36 mC/cm^2, starting with ODN **2**. They were anchored on to the Si ⊢COOH surface under near equilibrium conditions, using carbodiimide EDAC, $R_1N = C = NR_2$ mediated amidation in the presence of NHS as described in the literature (3,54,55). More precisely, this reaction involves several steps (http://chem.ch.huji.ac.il/~eugeniik/edc.htm), as outlined in Scheme 2. The carbodiimide is the promoter, which converts the acid into the O-acyl-urea intermediate (I); NHS is a catalyst that readily reacts with (I) affording the succinimidyl ester *in situ* (II); (II) is a well-known species, which has been detected on silicon surface with ATR-FTIR (55) and it has been also prepared and used *ex situ* in this process (3). The concentration of the immobilized ODN was then evaluated through enzymatic digestion with a DNase. To the best of our knowledge, this procedure was never applied before for a similar purpose. The only related reports (7,8) deal with the enzymatic removal of fluorescent ODNs, deposited as millimetre sized spots on gold surfaces,

and detected by fluorescence microscopy. It was claimed that, the digestion is complete in 3 h, at room temperature, with 20 U of enzyme. We used a lower enzyme amount and verified the completeness of the digestion by measuring the fluorescence of the solution over time. Fluorescence increased asymptotically towards a limiting value (Figure 2) and the digestion was apparently almost complete in 6 h. Then, other experiments were performed varying the concentration of the ODN-probe in the solution in contact with the layer of 10-undecynoic acid, in order to assess the minimal concentration necessary for attaining an optimal surface functionalization, and the concentration of the ODN-target in the solution in contact with the anchored ODN in the hybridization process, in order to assess the lowest ODN-target concentration giving maximal response (100% hybridization) through this procedure. As shown in Table 2, an ODN-probe density of 5.64×10^{12} strands/cm^2 can be considered optimal, and it resulted by reaction with probe-ODN at a concentration in solution 0.543 μM. The minimal ODN-target **3** concentration in solution, required for a 100% hybridization efficiency with ODN **2**, was 9.369 μM (Table 3). The LOD, (assumed as three times the noise level) was determined by further lowering the ODN-target **3** concentration, and resulted 0.312 μM. Other experiments were carried out with ODN (**1**,**5**,**7**), bearing the aminohexyl group, as probes. The overall results are reported in Table 4. After immobilization on identical supports (type A in Scheme 1), the surface concentrations of the 20mers ODN **1** and **5**, employing a solution concentration equal to the optimal value already established for **2** (0.54 μM), resulted (±ESD from three determinations) similar to each other and close to the optimal value found for ODN **2**: 5.63 ± 0.15 and $5.93 \pm 0.34 \times 10^{12}$ strands/cm^2, respectively. The 51mer **7** was used at concentrations in the solution in contact with the bound 10-undecynoic acid, up to 5.0 μM, but a surface concentration of only $1.97 \pm 0.34 \times 10^{12}$ strands/cm^2 resulted attainable, which however is still in the optimal loading range, as

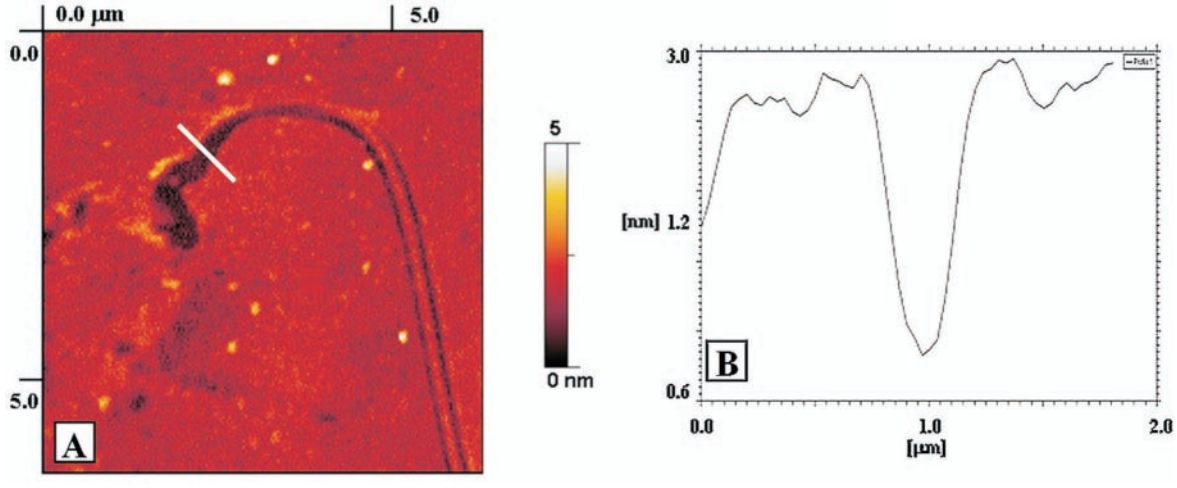

Figure 5. AFM tapping mode topographic image (**A**) (6 × 6 μm) of 10-undecynoic acid CEG deposited on Si(100) surface at 36 mC/cm^2 cathodic charge density and covered with a very low concentration of ssODN **2**. The non-functionalized area allows to define as ca. 1.5 nm the height of the 10-undecynoic acid layer on the surface. The ODN molecules are represented as small round structures. The white bar indicates the analysed zone. The cross section profile (**B**) is measured along the bar. It should be noted that the scratch profile line is fairly smooth, and the local corrugation of the monolayer is consistent with the uniform monolayer.

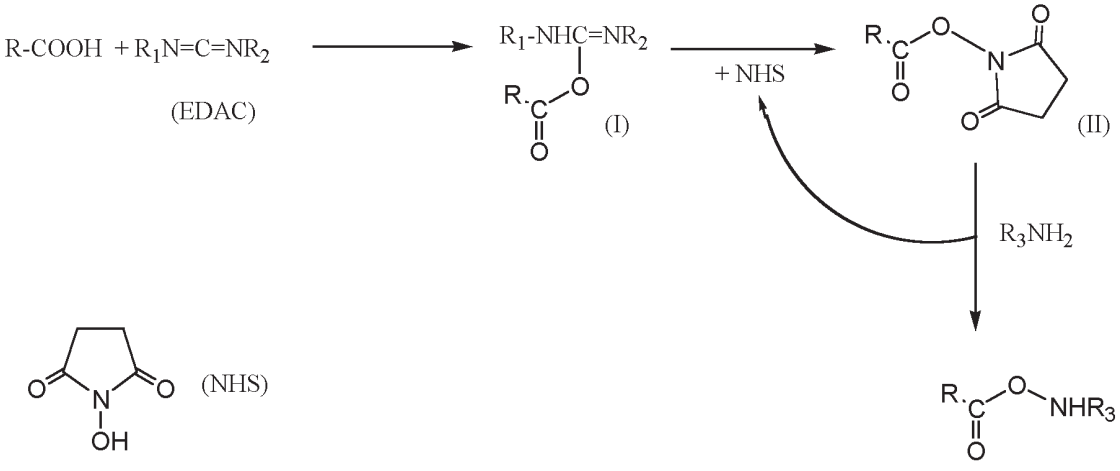

Scheme 2. Amidation reaction mechanism.

Table 4. Experimental data obtained with ODNs immobilized and hybridized on the silicon surface

Support	ODN (probe)	Concentration (μM)[a]	Reactant	Surface ODN concentration (10^{12} strands/cm^2)[b]	ODN (target)	Surface hybridized ODN concentration (10^{12} strands/cm^2)[c]
Si ⊢COOH	**1**	0.54	EDAC/NHS	5.63 ± 0.15	**2**	7.56 ± 0.28
Si ⊢COOH	**2**	0.54	EDAC/NHS	5.64 ± 0.15	**1**	5.64 ± 0.18
Si ⊢COOH	**5**	0.54	EDAC/NHS	5.93 ± 0.34	**6**	7.43 ± 0.80
Si ⊢COOH	**7**	5.0	EDAC/NHS	1.97 ± 0.16	**8**	2.78 ± 0.15
Si/SiO_2 ⊢OH	**2**	0.54	EDAC/NHS	0		
Si ⊢COOH	**1**	0.54	EDAC/NHS	0		
Si ⊢COOH	**1**	0.54	–	0		
Si ⊢COOH	**3**	0.54	EDAC/NHS	1.19 ± 0.15	**2**	0
Si ⊢COOH	**1**, **2**	0.54	EDAC/NHS	5.60 ± 0.20		0
Si ⊢COOH	**2**	0.54	EDAC/NHS	5.60	**6**	0

[a]ODN concentration in the loading solution.
[b]After enzymatic digestion and fluorescence measurement in solution.
[c]After denaturation and fluorescence measurement in solution.

discussed above, and proved able to hybridize efficiently (Table 4).

Furthermore, we performed several control experiments to confirm that the overall procedure is robust and takes place mainly in the specific way outlined in Scheme 1. To this end, in order to check whether immobilization can occur through simple adsorption, or through reaction with internal moieties of ODNs possibly involved in carbodiimide chemistry, e.g. the exocyclic amino or terminal hydroxyl groups, as found by other authors on glass supports (66), we tested ODN with either the linker arm (**1** and **2**) or without it (**3**), under different conditions, on different supports: (i) HO-terminated oxidized silicon (Si/SiO_2 ⊢OH) and **2** in the presence of EDAC/NHS; (ii) hydrogenated silicon (Si ⊢H) and **1** in the presence of EDAC/NHS; (iii) Si ⊢COOH and **1** without EDAC/NHS; (iv) Si ⊢COOH and **3** according to the standard, complete procedures. In experiment (iv), a small amount of ODN **3** proved to anchor on the surface, likely through the formation of amido bonds with its exocyclic amino groups, however it proved totally unable to hybridize. No control experiments other than (iv) with ODN **3** gave any detectable fluorescence signal, by operating with the ODNs at the optimal concentrations indicated above.

In order to verify the stability of the anchored ODNs to such hybridization procedure, the same was applied to two samples loaded with either ODN **1** or **2**, but without adding the respective complementary ODN, and no fluorescence was detected in any washing solution until Phosphodiesterase I was added. One further experiment was run in order to better evaluate the process of hybridization on the surface derivatized with probe-ODN **2**, performing the whole hybridization procedure and using as target the non-complementary fluorescein-labelled ODN **6**. No measurable fluorescence resulted other than in the washing solutions containing **6**.

To characterize the above preparations we report the tapping mode AFM imaging of a silicon sample covered first with 10-undecynoic acid (57) and then with ODN **1**, prepared according to the optimized procedure, at a nominal density of 5.63×10^{12} strands/cm^2, which displayed a homogeneous distribution of round structures (Figure 6; panels 1 and 2). A complication in determining the dimensions of these structures comes from the high packing of the layer, which results in a mean distance between adjacent ODNs around 5 nm. However, there are areas on the surface, where the intermolecular distance is statistically larger than the mean value allowing a simpler and reliable analysis. Following this strategy, we have focussed our efforts on these regions and measured a lateral dimension of ca. 18 nm and vertical height of ca. 3 nm.

Since the expected height of a 20mer ODN is slightly <7 nm (67), to understand the observed vertical dimensions of these structures one must take into account the mechanism of AFM imaging. The tip-sample interaction always produces a deformation of the sample. Ultra-soft molecules like ssODN can be considered as elastic rods (68), thus due to the probe-induced compression, their measured heights are lower than the expected molecule vertical dimensions. This effect is probably coupled with a non-vertical protrusion of the molecules over the surface, as predicted, for instance, for a 15mer ODN anchored on a flat gold surface, whose vertical height may change from 6.5 to 2.0 nm depending on the tilt angle formed between the normal to the surface and the vertical axis of the ODN (69). Indeed, the angular tilting of ODNs immobilized on gold, was recently investigated and it was supposed to be responsible of an apparent reduction of the observed ODN height: i.e. 3 nm instead of the predicted 16 nm for a completely elongated 25mer ODN (4). This could explain the low height values that we have measured.

Regarding the lateral dimensions, the structures appear wider than the width of a ssODN, ca. 2 nm as theoretically calculated (70). However, the measured widths are closer to the theoretical value than most of those recently reported, regarding similar specimens analysed in analogous conditions (71–73). In fact, the AFM technique intrinsically produces images in which the structures are the convolution of the imaged object with the tip shape and this effect is particularly evident when the probe has an apical radius larger than the lateral dimensions of the structures under analysis. These anomalously large dimensions can be then, attributed to the broadening effect due to the tip-sample convolution.

Hybridization trials were, then, carried out in triple on four different substrates (type B in Scheme 1), containing the probe-ODNs: Fluorescein-5′-dA_{20}-3′-Hexyl-NH_2 (**1**) or Fluorescein-5′-dT_{20}-3′-Hexyl-NH_2 (**2**), Fluorescein-5′-dX_{20}-3′-Hexyl-NH_2 (**5**) or Fluorescein-5′-dX_{51}-3′-Hexyl-NH_2 (**7**). In all four cases, high hybridization efficiency was obtained upon

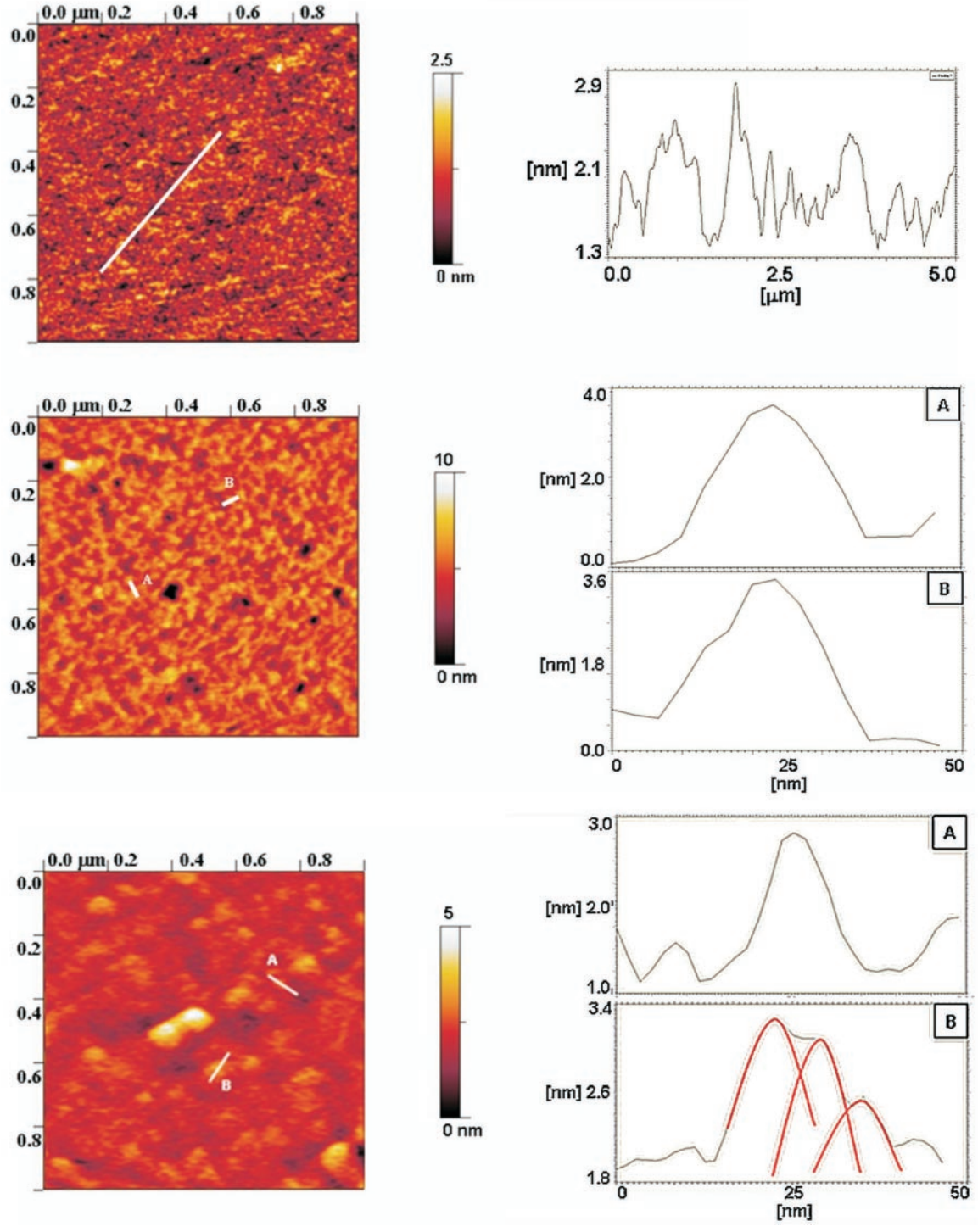

Figure 6. Panel 1: AFM tapping mode topographic image (1 × 1 µm) of a Si(100) surface covered with a uniform layer of 10-undecynoic acid using a CEG procedure at 120 mC/cm^2 cathodic charge density. The white bar indicates the analysed zone. The cross section evidences that the mean corrugation of the sample is around 1.3 nm. Panel 2: AFM tapping mode topographic image (1 × 1 µm) of a sample covered with 20mer ODN **1** (nominal density 5.63 × 10^{12} strands/cm^2). The cross sections A and B show structures ca. 18 nm wide and ca. 3 nm high. The white bar indicates the analysed zone. The vertical heights, as measured along the bars, are reported in A and B. Panel 3: AFM tapping mode topographic image (1 × 1 µm) of a sample covered with a dsODN **1** + **4** (nominal density 5.63 × 10^{12} strands/cm^2). The molecules appear as rod-like structures. Cross section A shows a structure ca. 20 nm wide and ca. 1.5 nm high. The height is lower than that of ssODN **1** (ca. 3 nm), probably due to a different orientation of the molecules on the surface. Cross section B, taken on a large agglomerate, can be deconstructed in three smaller structures with dimensions, shown by the fit curves, comparable with the dimensions of single molecules. The formation of large structures appears to be a side-effect of the hybridization process, as reported in the literature for similar samples (41). The white bar indicates the analysed zones. The cross section profiles as measured along the bar, without and with deconvolution of the profile, are reported in A and B, respectively.

interaction with the corresponding complementary ODNs, prepared according to the optimized procedure: Fluorescein-5′-dT_{20} (**4**), Fluorescein-5′-dA_{20} (**3**), Fluorescein-5′-dX_{20} (**6**) and Fluoresceine-5′-dX_{24} (**8**), respectively, as resulted by the subsequent denaturation of the hybrids reported in Table 4. The anchored ODNs **1**, **2**, **5** and **7** were then finally digested with Phosphodiesterase I and their amounts were compared with those of the hybridized **3**, **4**, **6** and **8**, resulting practically equivalent within the ESD. Nevertheless, the systematically higher values of the hybridized ODNs, with respect to the bound ODNs, may reflect a limited ability of the DNase to completely digest the ODNs anchored on the surface.

Similarly as above, Figure 6; panel 3 shows the tapping mode AFM image of a typical ODN sample after hybridization (namely **1** + **4**) using standard tips. The sample appears covered with small rod-like structures and some larger structures of various dimensions. The lateral dimensions of the smaller structures of the dsODNs on the surface result ca. 20 nm and their vertical dimensions ca. 1.5 nm (Cross section A of Figure 6; panel 3). The increase of the size observed for the dsODNs structures, compared to the analogous ss, can be attributed to the effect of hybridization. A similar size increase was already reported on similar samples, e.g. 16mer ODN-probes on oxidized silicon surface (41). The different vertical dimensions can be interpreted as consequence of the different tilting of the ODN with respect to the surface which could also justify their apparent greater mean lateral dimension.

One of the larger structures shown in Figure 6; panel 3 displays an estimated width of ca. 80 nm and this can be attributed to an apparent aggregation of smaller dsODNs structures. This is shown in the cross section profile B of Figure 6; panel 3, where the large structure has been tentatively fitted as the aggregation of three smaller (ca. 20 nm) ones, whose dimensions are compatible with the single rod-like structures.

With the aim to assess the convolution effect mentioned above, and to confirm our ability to detect single ssODNs, we also acquired some images using high resolution tips. These 'super-tips' have an apical radius of ca. 2 nm, thus the convolution has a much weaker impact on the lateral dimensions of the ODNs (74). In Figure 7; panel 1, we show a sample covered with a low density (nominal density ca. 10^{11} strands/cm^2) of ODN **1**. The use of this low ODN density determines a large (ca. 30 nm) mean space between the molecules. In this case the ssODN molecules appear as round structures with width of ca. 8 nm and height of ca. 1.8 nm. The different vertical dimensions are explainable considering that the same probe force generates an higher pressure when applied

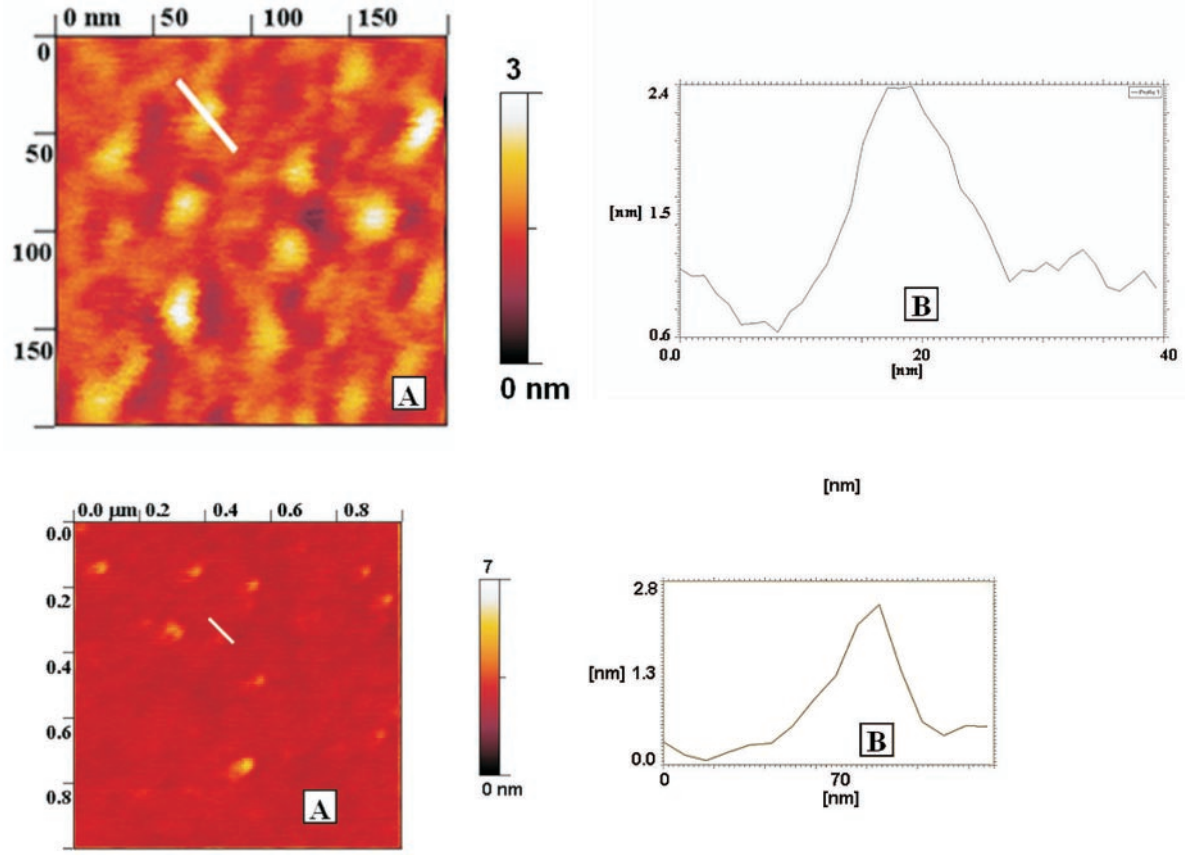

Figure 7. Panel 1: AFM tapping mode topographic image (**A**), (250 × 250 nm) of a sample covered with a low concentration (nominal density ca. 10^{11} strands/cm^2) of 20mer ODN **1**, acquired by the use of super-tips (apical radius ca. 2 nm). The cross section shows a structure ca. 8 nm wide and ca. 1.8 nm high. The different lateral dimensions of these structures compared with the samples analysed with the standard tips (apical radius ca. 30 nm) illustrates the importance of the apical radius and form. The different vertical dimensions are probably the effect of the greater tip pressure due to the much smaller contact area. The white bar indicates the analysed zone. The cross section profile, as measured along the bar, is reported in (B). Panel 2: AFM tapping mode topographic image (**A**), (1 × 1 µm) of a sample covered with a very low concentration (nominal density around 10^{10} strands/cm^2) of 20mer ODN **1**. The low concentration allows to unequivocally analyse every single molecule. The white bar indicates the analysed zone. The cross section (B) shows that the structures are ca. 25 nm wide and ca. 2.5 nm high.

on a smaller interaction area, thus producing a larger deformation and possibly enhancing the angular tilt of the molecules on the surface. In both low and high resolution images, the surface between each structure is uniform and has a corrugation comparable with a clean silicon surface functionalized with 10-undecynoic acid.

Furthermore we performed measurements using standard tips on another sample covered at a low nominal density, around 10^{10} strands/cm^2 of the 20mer ODN **1**. This was done in order to show that the features observed with the super-tips would appear with a larger lateral size if imaged using the standard tips. The use of such a low ODN density determines an even larger mean space between the molecules, allowing to undoubtedly discriminate the single molecules even using the standard tips. This is reported in Figure 7; panel 2. As a major consequence of the analogy of the observed dimensions we can claim that the structures are the same as observed in Figure 6; panel 2 (standard tip/high concentration). Thus, we demonstrated the single molecule sensitivity and obtained a state-of-the-art lateral resolution of 8.6 nm.

CONCLUSIONS

A simple, robust, accurate and optimized two-step procedure to functionalize unoxidized crystalline silicon, Si(100), with controlled amounts of ODNs is hereby reported. The samples produced through this procedure have been exploited as probe systems for DNA recognition.

First, 10-undecynoic acid was covalently anchored on the silicon surface, via CEG, attaining a carboxylic acid terminated monolayer upon passage of 36 mC/cm^2 charge density. Then, ssODNs were immobilized on this layer via amidation. The concentration of both ssODNs and dsODNs were determined through fluorescence measurements in solution. This procedure allowed us (i) to assess the optimal-probe density, for 20mer ODNs, on the surface ($5–6 \times 10^{12}$ strands/cm^2), i.e. the maximum loading which yields a 100% hybridization efficiency and (ii) to determine the corresponding ODN-target LOD (0.312 μM). One longer (50mer) ODN tested, lead to lower loading, still maintaining however the ability to fully hybridize. AFM has proved a useful tool to characterize the whole procedure by parallel imaging.

Samples prepared in this way, using crystalline silicon, are good candidates for the development of new, label-free, ultrasensitive biosensor devices based on a change in electrical properties associated with biorecognition events occurring at their surface.

ACKNOWLEDGEMENTS

This work was carried out in part with the financial support of MIUR, FIRS project. Thanks go also to Prof. G. Marletta for continuous encouragement. Funding to pay the Open Access publication charges for this article was provided by CNR.

Conflict of interest statement. None declared.

REFERENCES

1. Ball,P. (2005) Silicon still supreme. *Nature Mater*., **4**, 119.
2. Hersam,M.C., Guisinger,N.P. and Lydin,J.W. (2000) Silicon-based molecular nanotechnology. *Nanotechnology*, **11**, 70–76.
3. Yin,H.B., Brown,T., Greef,R., Wilkinson,J.S. and J.Melvin,J. (2004) Chemical modification and micropatterning of Si(100) with oligonucleotides. *Microelectronic Eng*., **73–74**, 830–836.
4. Herne,T.M. and Tarlov,M.J. (1997) Characterization of DNA probes immobilized on gold surfaces. *J. Am. Chem. Soc*., **119**, 8916–8920.
5. Peterlinz,K.A. and R.M.Georgiadis,R.M. (1997) Observation of hybridisation and dehybridisation of thiol-tethered DNA using two-color surface plasmon resonance spectroscopy. *J. Am. Chem. Soc*., **119**, 3401–3402.
6. Jordan,C.E., Frutos,A.G., Thiel,A.J. and Corn,R.M. (1997) Surface plasmon resonance imaging measurements of DNA hybridisation adsorption and streptavidin/DNA multilayer formation at chemically modified gold surfaces. *Anal. Chem*., **69**, 4939–4947.
7. Frutos,A.G., Liu,Q., Thiel,A.J., Sanner,A.M.W., Condon,A.E., Smith,L.M. and Corn,R.M. (1997) Demonstration of a word design strategy for DNA computing on surfaces. *Nucleic Acids Res*., **25**, 4748–4757.
8. Frutos,A.G., Smith,L.M. and Corn,R.M. (1998) Enzymatic ligation reactions of DNA 'word' on surfaces for DNA computing. *J. Am. Chem. Soc*., **120**, 10277–10282.
9. Yang,M., Yau,H.C.M. and Chan,H.L. (1998) Adsorption kinetics and ligand-binding properties of thiol-modified double-stranded DNA on a gold surface. *Langmuir*, **14**, 6121–6129.
10. Steel,A.B., Herne,T.M. and Tarlov,M.J. (1998) Electrochemical quantitation of DNA immobilized on gold. *Anal. Chem*., **70**, 4670–4677.
11. Levicky,R., Herne,T.M., Tarlov,M.J. and Satija,S.K. (1998) Using self-assembling to control the structure of DNA monolayers on gold: a neutron reflectivity study. *J. Am. Chem. Soc*., **120**, 9787–9792.
12. Brockman,J.M., Frutos,A.G. and Corn,R.M. (1999) A multistep chemical modification procedure to create DNA arrays on gold surfaces for the study of protein-DNA interactions with surface plasmon resonance imaging. *J. Am. Chem. Soc*., **121**, 8044–8051.
13. Demers,L.M., Mirkin,C.A., Mucic,R.C., Reynolds,R.A., Letsinger,R.L., Elghanian,R. and Viswanadham,G. (2000) A fluorescence-based method for determining the surface coverage and hybridisation efficiency of thiol-capped oligonucleotides bound to gold thin films and nanoparticles. *Anal. Chem*., **72**, 5535–5541.
14. Smith,E.A., Wanat,M.J., Cheng,Y., Barreira,S.V.P., Frutos,A.G. and Corn,R.M. (2001) Formation, spectroscopy characterization, and application of sulfhydryl-terminated alkanethiol monolayers for the chemical attachment of DNA onto gold surfaces. *Langmuir*, **17**, 2502–2507.
15. Weizmann,Y., Patolsky,F. and Willner,I. (2001) Amplified detection of DNA and analysis of single-base mismatches by the catalyzed deposition of gold on Au-nanoparticles. *Analyst*, **126**, 1502–1504.
16. Peterson,A.W., Heaton,R.J. and Georgiadis,R.M. (2001) The effect of surface probe density on DNA hybridisation. *Nucleic Acids Res*., **29**, 5163–5168.
17. Peterson,A.W., Wolf,L.K. and Georgiadis,R.M. (2002) Hybridisation of mismatched or partially matched DNA at surfaces. *J. Am. Chem. Soc*., **124**, 14601–14607.
18. Yu,H.Z., Luo,C.Y., Sankar,C.G. and Sen,D. (2003) Voltammetric procedure for examining DNA-modified surfaces: quantitation, cationic binding activity, and electron-transfer kinetics. *Anal. Chem*., **75**, 3902–3907.
19. Wirtz,R., Wälti,C., Germishuizen,W.A., Pepper,M., Middelberg,A.P.J. and Davies,A.G. (2003) High-sensitivity colorimetric detection of DNA hybridisation on a gold surface with high spatial resolution. *Nanotechnology*, **14**, 7–10.
20. Shumaker-Parry,J.S., Zareie,M.H., Aebersold,R. and Campbell,C.T. (2004) Microspotting streptavidin and double-stranded DNA arrays on gold for high-throughput studies of protein-DNA interactions by surface plasmon resonance microscopy. *Anal. Chem*., **76**, 918–929.
21. Guiducci,C., Stagni,C., Zuccheri,G., Bogliolo,A., Benini,L., Samorì,B. and Riccò,B. (2004) DNA detection by integrable electronics. *Biosens. Bioelectron*., **19**, 781–787.
22. Yu,F., Yao,D. and Knoll,W. (2004) Oligonucleotide hybridisation studied by a surface plasmon diffraction sensor (SPDS). *Nucleic Acids Res*., **32**, e75.
23. Maskos,U. and Southern,E.M. (1992) Oligonucleotide hybridisations on glass supports: a novel linker for oligonucleotide synthesis and hybridisation properties of oligonucleotides synthesised *in situ*. *Nucleic Acids Res*., **7**, 1679–1684.

24. Guo,Z., Guifoyle,R.A., Thiel,A.J., Wang,R. and Smith,L.M. (1994) Direct fluorescence analysis of genetic polymorphisms by hybridisation with oligonucleotide arrays on glass supports. *Nucleic Acids Res.*, **22**, 5456–5465.
25. Vo-Dinh,T., Alarie,J.P., Isola,N., Landis,D., Wintenberg,A.L. and Ericson,M.N. (1999) DNA biochip using a phototransistor integrated circuit. *Anal. Chem.*, **71**, 358–363.
26. Zammatteo,N., Jeanmart,L., Hamels,S., Courtois,S., Louette,P., Hevesi,L. and Remacle,R. (2000) Comparison between different strategies of covalent attachment of DNA to glass surfaces to build DNA microarrays. *Anal. Biochem.*, **280**, 143–150.
27. Podyminogin,M.A., Lukhtanov,E.A. and Reed,M.W. (2001) Attachment of benzaldehyde-modified oligodeoxynucleotide probes to semicarbazide-coated glass. *Nucleic Acids Res.*, **29**, 5090–5098.
28. Oh,S.J., Cho,S.J., Kim,C.O. and Park,J.W. (2002) Characteristics of DNA microarrays fabricated on various aminosilane layers. *Langmuir*, **18**, 1764–1769.
29. Cerrina,F., Blattner,F., Huang,W., Hue,Y., Green,R., Singh-Gasson,S. and Sussman,M. (2002) Biological lithography: development of a maskless microarray synthesizer for DNA chips. *Microelectronic Eng.*, **61–62**, 33–40.
30. Albert,T.J., Norton,J., Ott,M., Richmond,T., Nuwaysir,K., Nuwaysir,E.F., Stengele,K.P. and Green,R.D. (2003) Light-directed 5′→3′ synthesis of complex oligonucleotide microarrays. *Nucleic Acids Res.*, **31**, e35.
31. Kumar,P., Choithani,J. and Gupta,K.C. (2004) Construction of oligonucleotide arrays on a glass surface using a heterobifunctional reagent, N-(2-trifluoroethanesulfonatoethyl)-N- (methyl)-triethoxysilylpropyl-3-amine (NTMTA). *Nucleic Acids Res.*, **32**, e80.
32. Pirri,G., Damin,F., Chiari,M., Bontempi,E. and Depero,L.E. (2004) Characterization of a polymeric adsorbed coating for DNA microarray glass slides. *Anal. Chem.*, **76**, 1352–1358.
33. Lamture,J.B., Beattie,K.L., Burke,B.E., Eggers,M.D., Ehrlich,D.J., Fowler,R., Hollis,M.A., Kosicki,B.B., Reich,R.K., Smith,S.R., Varma,R.S. and Hoga,M.E. (1994) Direct detection of nucleic acid hybridisation on the surface of a charge couplet device. *Nucleic Acids Res.*, **22**, 2121–2125.
34. Lee,G.U., Chrisey,L.A. and Colton,R.J. (1994) Direct measurement of the force between complementary strands of DNA. *Science*, **266**, 771–773.
35. Jin,L., Horgan,A. and Levicky,R. (2003) Preparation of end-tethered DNA monolayers on siliceous surfaces using heterobifunctional cross-linker. *Langmuir*, **19**, 6968–6975.
36. Shen,G., Anand,M.F.G. and Levicky,R. (2004) X-ray photoelectron spectroscopy and infrared spectroscopy study of maleimide-activated supports for immobilization of oligodeoxyribonucleotides. *Nucleic Acids Res.*, **32**, 5973–5980.
37. Xu,J., Zhu,J.J., Huang,Q. and Chen,H.Y. (2001) A novel DNA-modified indium tin oxide electrode. *Electrochemistry Comm.*, **3**, 665–669.
38. Gray,D.E., Case-Green,S.C., Fell,T.S., Dobson,P.J. and Southern,E.M. (1997) Ellipsometric and interferometric characterization of DNA probes immobilized on a combinatorial array. *Langmuir*, **13**, 2833–2842.
39. O'Donnell,M.J., Tang,K., Köster,H., Smith,C.L. and Cantor,C.R. (1997) High-density, covalent attachment of DNA to silicon wafers for analysis by MALDI-TOF mass spectrometry. *Anal. Chem.*, **69**, 2438–2443.
40. Berney,H., West,J., Haefele,E., Alderman,J., Lane,W. and Collins,J.K. (2000) A DNA diagnostic biosensor: development, characterization and performance. *Sens. Actuators B Chem.*, **68**, 100–108.
41. Lenigk,R., Carles,M., Ip,N.Y. and Sucher,N.J. (2001) Surface characterization of a silicon-chip based DNA microarray. *Langmuir*, **17**, 2497–2501.
42. Cavic,B.A., McGovern,M.E., Nisman,R. and Thompson,M. (2001) High surface density immobilization of oligonucleotide on silicon. *Analyst*, **126**, 485–490.
43. Li,Z., Chen,Y., Li,X., Kamins,T.I., Nauka,K. and Williams,R.S. (2004) Sequence-specific label-free DNA sensors based on silicon nanowires. *Nano Lett.*, **4**, 245–247.
44. Macanovic,A., Marquette,C., Polychronakos,C. and Lawrence,M.F. (2004) Impedance-based detection of DNA sequences using a silicon transducer with PNA as the probe layer. *Nucleic Acids Res.*, **32**, e20.
45. Meinkoth,J. and Wahl,G. (1984) Hybridisation of nucleic acids immobilized on solid supports. *Anal. Biochem.*, **138**, 267–284.
46. Gingeras,T.R., Kwoh,D.Y. and Davis,G.R. (1987) Hybridisation properties of immobilized nucleic acids. *Nucleic Acids Res.*, **15**, 5373–5390.
47. Lund,V., Schmid,R., Rickwood,D. and Hornes,E. (1988) Assessment of methods for covalent binding of nucleic acids to magnetic beads, Dynabeads, and the characteristics of the bound nucleic acids in hybridisation reactions. *Nucleic Acids Res.*, **16**, 10861–10880.
48. Saiki,R.K., Walsh,P.S., Levenson,C.H. and Erlich,H.A. (1989) Genetic analysis of amplified DNA with immobilized sequence-specific oligonucleotide probes. *Proc. Natl Acad. Sci. USA*, **86**, 6230–6234.
49. Rasmussen,S.R., Larsen,M.R. and Rasmussen,S.E. (1991) Covalent immobilization of DNA onto polystyrene microwells: the molecules are only bound at the 5′ end. *Anal. Biochem.*, **198**, 138–142.
50. Zhang,Y., Coyne,M.Y., Will,S.G., Levenson,C.H. and Kawasaki,E.S. (1991) Single-base mutational analysis of cancer and genetic diseases using membranes bound modified oligonucleotides. *Nucleic Acids Res.*, **19**, 3929–3933.
51. Strother,T., Hamers,R.J. and Smith,L.M. (2000) Covalent attachment of oligodeoxyribonucleotides to amine-modified Si (001) surfaces. *Nucleic Acids Res.*, **28**, 3535–3541.
52. Strother,T., Cai,W., Zhao,X., Hamers,R.J. and Smith,L.M. (2000) Synthesis and characterization of DNA-modified silicon (111). *J. Am. Chem. Soc.*, **122**, 1205–1209.
53. Patole,S.N., Pike,A.R., Connolly,B.A., Horrocks,B.J. and Houlton,A. (2003) STM study of DNA films synthesized on Si (111) surfaces. *Langmuir*, **19**, 5457–5463.
54. Wei,F., Sun,B., Guo,Y. and Zhao,X.S. (2003) Monitoring DNA hybridisation on alkyl modified silicon surface through capacitance measurement. *Biosens. Bioelectron.*, **18**, 1157–1163.
55. Voicu,R., Boukherroub,R., Bartzoka,V., Ward,T., Wojtyk,J.T.C. and Wayner,D.D.M. (2004) Formation, characterization, and chemistry of undecanoic acid-terminated silicon surfaces: patterning and immobilization of DNA. *Langmuir*, **20**, 11713–11720.
56. Cai,W., Peck,J.R., van der Weide,D.W. and Hamers,R.J. (2004) Direct electrical detection of hybridisation at DNA-modified silicon surfaces. *Biosens. Bioelectron.*, **19**, 1013–1019.
57. Cattaruzza,F., Cricenti,A., Flamini,A., Girasole,M., Longo,G., Mezzi,A. and Prosperi,T. (2004) Carboxylic acid terminated monolayer formation on cristalline silicon and silicon nitride surfaces. A surface coverage determination with a fluorescent probe in solution. *J. Mater. Chem.*, **14**, 1461–1468.
58. Cricenti,A., Generosi,R., Barchesi,C., Luce,M. and Rinaldi,M. (1998) A multipurpose scanning near-field optical microscope: reflectivity and photocurrent on semiconductor and biological samples. *Rev. Sci. Instrum.*, **69**, 3240–3244.
59. Wang,L., Gaigalas,A.K., Blasic,J. and Holden,M.J. (2004) Spectroscopic characterization of fluorescein- and tetramethylrhodamine-labeled oligonucleotides and their complexes with a DNA template. *Spectrochimica Acta, Part A*, **60**, 2741–2750.
60. Kelley,S.O., Jackson,N.M., Hill,M.G. and Barton,J.K. (1999) Long-range electron transfer through DNA films. *Angew. Chem. Int. Ed. Engl.*, **38**, 941–945.
61. Rosa-Zeiser,A., Weilandt,E., Hild,S. and Marti,O. (1997) The simultaneous measurement of elastic, electrostatic and adhesive properties by scanning force microscopy: pulsed-force mode operation. *Meas. Sci. Technol.*, **8**, 1333–1338.
62. Zhong,Q., Inniss,D., Kjoller,K. and Elings,V.B. (1993) Fractured polymer/silica fiber surface studied by tapping mode atomic force microscopy. *Surf. Sci.*, **290**, L688–L692.
63. Hong,B.J., Sunkara,V. and Park,J.W. (2005) DNA microarrays on nanoscale-controlled surface. *Nucleic Acids Res.*, **33**, e106.
64. Robins,E.G., Stewart,M.P. and Buriak,J.M (1999) Anodic and cathodic electrografting of alkynes on porous silicon. *Chem. Comm.*, 2479–2480.
65. Condorelli,C.G., Motta,A., Fragalà,I.L., Giannazzo,F., Raineri,V., Caneschi,A. and Gatteschi,D. (2004) Anchoring molecular magnets on Si(100) surface. *Angew. Chem. Int. Ed. Engl.*, **116**, 4173–4176.
66. Adessi,C., Matton,G., Ayala,G., Turcatti,G., Mermod,J.J., Mayer,P. and Kawashima,E. (2000) Solid phase DNA amplification: characterization of primer attachment and amplification mechanisms. *Nucleic Acid Res.*, **28**, e87.
67. Sinden,R. (1994), *DNA structure and function.* Academic Press, San Diego, CA, p. 23.

68. Morii,T., Mizuno,R., Haruta,H. and Okada,T. (2004) An AFM study of the elasticity of DNA molecules. *Thin Solid Films*, **464–465**, 456–458.
69. Kelley,O.S., Barton,J.K., Jackson,M.N., McPherson,D.L., Potter,A.B., Spain,E.M., Allen,J.M. and Hill,M.G. (1998) Orienting DNA helices on gold using applied electric fields. *Langmuir*, **14**, 6781–6784.
70. Lenninger,A.L., Nelson,D.L. and Cox,M.M. (1993) *Principles of Biochemistry*. Worth Publishers, NY, p. 334.
71. Huang,E., Zhou,F. and Deng,L. (2000) Studies of surface coverage and orientation of DNA molecules immobilized onto preformed alkanethiol self-assembled monolayers. *Langmuir*, **16**, 3272–3280.
72. Kossek,S., Padeste,C., Tiefenauer,L.X. and Siegenthaler,H. (1998) Localization of individual biomolecules on sensor surfaces. *Biosens. Bioelectron.*, **13**, 31–43.
73. Rouillat,M.H., Dugas,V., Martin,J.R. and Phaner-Goutorbe,M. (2005) Characterization of DNA chips on the molecular scale before and after hybridisation with an atomic force microscope. *Appl. Surf. Sci*, **252**, 1765–1771.
74. Bustamante,C., Vesenka,J., Tang,C.L., Rees,W., Guthold,M. and Keller,R. (1992) Circular DNA molecules imaged in air by scanning force microscopy. *Biochemistry*, **31**, 22–26.